Cerebral Cortex, 2017; 1–12

doi: 10.1093/cercor/bhw416
Original Article

ORIGINAL ARTICLE

The Rich-Club Organization in Rat Functional Brain Network to Balance Between Communication Cost and Efficiency

Xia Liang[1,2], Li-Ming Hsu[1,3], Hanbing Lu[1], Akira Sumiyoshi[1,4], Yong He[5] and Yihong Yang[1]

[1]Neuroimaging Research Branch, National Institute on Drug Abuse, Baltimore, MD 21224, USA, [2]Research Center of Basic Space Science, Harbin Institute of Technology, Harbin 150001, China, [3]Department of Biomedical Imaging and Radiological Sciences, National Yang-Ming University, Taipei 11221, Taiwan, [4]Institute of Development, Aging and Cancer, Tohoku University, Sendai 9808575, Japan and [5]State Key Laboratory of Cognitive Neuroscience and Learning, IDG/McGovern Institute for Brain Research, Beijing Normal University, Beijing 100875, China

Address correspondence to Yong He, State Key Laboratory of Cognitive Neuroscience and Learning, IDG/McGovern Institute for Brain Research, Beijing Normal University, Beijing 100875, China. Email: yong.he@bnu.edu.cn; Yihong Yang, Neuroimaging Research Branch, National Institute on Drug Abuse, National Institutes of Health, Baltimore, MD 21224, USA. Email: yihongyang@intra.nida.nih.gov.

Abstract

Network analyses of structural connectivity in the brain have highlighted a set of highly connected hubs that are densely interconnected, forming a "rich-club" substrate in diverse species. Here, we demonstrate the existence of rich-club organization in functional brain networks of rats. Densely interconnected rich-club regions are found to be distributed in multiple brain modules, with the majority located within the putative default mode network. Rich-club members exhibit high wiring cost (as measured by connection distance) and high metabolic running cost (as surrogated by cerebral blood flow), which may have evolved to achieve high network communications to support efficient brain functions. Furthermore, by adopting a forepaw electrical stimulation paradigm, we find that the rich-club organization of the rat functional network remains almost the same as in the resting state, whereas path motif analysis reveals significant differences, suggesting the rat brain reorganizes its topological routes by increasing locally oriented shortcuts but reducing rich-club member-involved paths to conserve metabolic running cost during unimodal stimulation. Together, our results suggest that the neuronal system is organized and dynamically operated in an economic way to balance between cost minimization and topological/functional efficiency.

Key words: functional connectome, module, motif, rat brain, rich club

Introduction

The brain can be modeled as a complex network of structurally connected and functionally interacting neuronal elements, organized to achieve an optimal balance between functional segregation and integration supporting efficient brain functions (Bullmore and Sporns 2009). While functional "segregation" is enabled by forming densely connected local communities, functional "integration" is achieved by global communication between distributed communities (Sporns 2013). The existence of densely connected and highly centralized brain network hubs, and their strong tendency to be mutually connected to form a "rich-club" core may play a crucial role in promoting

global communication and information integration (van den Heuvel and Sporns 2011, 2013a, 2013b; Harriger et al. 2012; Senden et al. 2014). Specifically, a recent study has demonstrated that the rich-club regions and their connections in the structural networks of the human brain might serve as a connectivity backbone (van den Heuvel et al. 2012), which allows information to be efficiently transferred between distant and peripheral regions or communities by taking express routes via the brain network hubs. Efficient global information processing may require costly infrastructure and operation of network hubs and rich-club connections, such as long-distance wiring connecting distant regions and high metabolic consumption by brain hubs (van den Heuvel et al. 2012; Liang et al. 2013; Collin et al. 2014b).

While brain hubs and rich-club architecture in humans (van den Heuvel and Sporns 2011, 2013a, 2013b; van den Heuvel et al. 2012) and their implications in neuropsychiatric disorders (van den Heuvel et al. 2013; Collin et al. 2014a; Dai et al. 2014) have been extensively explored in recent years, studies in rodents begun to investigate such network organization and demonstrated the existence of rich-club organization for structural brain connectome in both rats (Bota et al. 2015; van den Heuvel et al. 2015) and mice (Rubinov et al. 2015). These studies in rodent's brain provide topological organization of the structural brain network; however, brain hubs and rich-club structure in functional brain network of rodents still need to be thoroughly investigated. Specific questions include where the hub regions are located in the rodent functional brain network, whether the hubs are densely interconnected to form an expressway for efficient global information transferring, and what the costs are for wiring and running such a rich-club structure.

Another intriguing question is whether the rich-club organization will undergo changes when the brain responds to external stimulations. Unlike the relatively static structural brain connectome, functional brain networks can evolve dynamically in response to external stimuli or during task performance (Liang et al. 2015), which allows for investigation on whether and how the rich-club organization is modulated during specific stimulations. Exploring the reorganization principle of the rich-club structure is of great importance for understanding its functional implications in the neural systems, which still remains largely unclear due to relatively less studies of functional brain networks in rats and technical limitations to conduct stimulation experiments in anesthetized rats.

The organizational principle of functional brain networks and disruption in animal models of human diseases may hold potential for understanding human brain disorders from a network perspective and translating findings from animal models to humans. In the current study, using the rat imaging model developed by our group (Lu et al. 2012), we collected resting-state functional magnetic resonance imaging (MRI) data in rats and constructed their functional brain networks. We aimed to systematically assess rich-club organization in the rat functional brain architecture, including its spatial distribution in brain networks, communication cost (connection distance and metabolic expense as surrogated by cerebral blood flow [CBF]) and efficiency (general description of being efficient, rather than specific meaning in graph-theory), and information-transfer patterns across the brain. More importantly, to explore potential modulation effects of external stimulation on rich-club organization, we employed forepaw electrical stimulation experiment to explore reorganization principles of rich-club structure of rat functional brain networks in response to a unimodal external stimulation.

Materials and Methods

Animal Preparation

Twenty-seven male Sprague-Dawley rats (Charles River Laboratories) were used in the study. Rats weighed 275 ± 25 g upon arrival and were housed 2 per cage with ad libitum access to food and water. All animal procedures were approved by the Animal Care and Use Committee of the National Institute on Drug Abuse-Intramural Research Program.

For MRI scans, animals were anesthetized with a combination of isoflurane (Piramal Critical Care Inc.) and dexmedetomidine hydrochloride (Webster Veterinary Supply), in a protocol based on our previous study (Lu et al. 2012). Briefly, following a 0.03-mg/kg subcutaneous bolus injection, dexmedetomidine was continuously infused at 0.015 mg/kg/h and isoflurane was gradually reduced from 2% to 0.5%. Rats were secured in an animal holder with a bite bar. Core body temperature was maintained at 37 ± 0.5 °C with a water-circulating heating pump. Heart rate, respiration rate, and blood oxygenation levels were continuously monitored using a noninvasive pulse oximetry attached to the animal's hind foot (Starr Life Sciences). Spontaneous respiration rate typically ranged from 70 to 85 breaths/min at the time of resting-state data acquisition. Functional magnetic resonance imaging (fMRI) data were collected at approximately 90 min after the initiation of dexmedetomidine infusion, at which time the blood-oxygen-level dependence (BOLD) signal was maximally stable (Lu et al. 2012). During electrical forepaw stimulations, 2 needle electrodes were placed under the skin of the left forepaw which sending the electrical stimulation in a block-design pattern with 3 cycles of 20-s on and 40-s off. An electrical stimulator (Model S88, Grass Instrument Co.) was used to deliver electrical pulses (current: 3 mA, pulse duration: 0.3 ms, frequency: 9 Hz).

Image Acquisition

MRI data were acquired using a Bruker Biospin 9.4 T scanner (Bruker Medizintechnik) with a quadrature receiver coil and birdcage volume transmit coil. For each rat, high-resolution anatomical image, resting-state fMRI and electrical forepaw stimulation fMRI were acquired. The MRI data used in the current study would be available through a Data Transfer Agreement under current policies of NIH.

High-resolution anatomical images were acquired using a Rapid Acquisition with Relaxation Enhancement (RARE) sequence (repetition time [TR] = 2500 ms, FOV = 32 × 32 mm^2, slice thickness = 1 mm, slice number = 23). Resting fMRI scan was acquired using a T2*-weighted EPI sequence (TE = 15 ms, TR = 1000 ms, FOV = 30 × 30 mm^2, matrix size = 64 × 64, slice thickness = 1 mm, slice number = 13, time points = 520). We also acquired an fMRI scan under electrical forepaw stimulation (acquisition parameters as above with time points = 200). During the stimulation scan, 2 needle electrodes were placed under the skin of the left forepaw, which set the electrical stimulation in a block-design pattern with 3 cycles of 20-s on and 40-s off. An electrical stimulator (Model S88, Grass Instrument Co., Quincy, MA) was used to deliver electrical pulses (current: 3 mA, pulse duration: 0.3 ms, frequency: 9 Hz).

Functional arterial spin labeling (ASL) data were acquired in another 8 anesthetized rats. Interleaved control and label images were acquired using a gradient echo EPI sequence with TR = 9.6 s, TE = 12 ms, 7 1.5 mm slices, FOV = 3.2 × 3.2 cm^2, matrix size = 64 × 64, labeling duration = 1.2 s. Sixty labeling-control pairs were acquired to enhance the signal noise ratio. No postlabeling delay between the labeling pulse and the slice

excitation pulse was employed ($w = 0$). Instead, bipolar diffusion weighting gradients were simultaneously applied along X, Y and Z ($b = 149\,s/mm^2$) to minimize ASL signal originating from relatively large arteries.

Data Preprocessing

fMRI data were preprocessed using AFNI (Cox and Hyde 1997). For resting and forepaw stimulation fMRI data, preprocessing steps included discarding the first 10 volumes, slice timing correction, motion correction, and spatial smoothing (full-width at half-maximum [FWHM], 0.6 mm). For spatial normalization, first, we created a study-specific averaged high-resolution anatomical image by registering the T_1-weighted image of each rat to a representative animal's T_1 image, and then averaging the registered images across rats. The averaged T_1 image was then affine transformed to the minimal deformation template (MDT) generated by Valdés-Hernández et al. (2011). For each animal, fMRI images were then brought to MDT space by applying the catenated transforms of fMRI images to the corresponding T_1-weighted image, then to the averaged T_1 image, and finally to the MDT template. The normalized images were then linearly detrended and temporal filtered (high-pass filter of 0.01 Hz), and the 6 head motion parameters, along with averaged signals from white matter and ventricles were removed by multiple regressing analysis.

For forepaw stimulation data, subject-specific responses were modeled using a general linear model (GLM) that included a boxcar function convolved with a canonical hemodynamic response function, modeling stimulus-bound processing. A one-sample *t*-test was performed to detect activated brain regions at a group level ($P < 0.0001$, corrected).

ASL data were preprocessed as follows. After spatial smoothing (FWHM = 0.9 mm), CBF-weighted time series were created by pairwise subtraction of the label and control images. Then, absolute regional cerebral blood flow (rCBF) time series were approximated using a one-compartment model, and averaged together to get individual-level absolute rCBF maps. Finally, rCBF maps were aligned to their corresponding T_1-weighted images and then normalized by applying the above-mentioned transformation of T_1-weighted images to MDT template.

Image Analyses

Network Construction

To construct rat brain functional network, we first parcellated the rat brain into 110 regions by combining atlases as provided by Valdés-Hernández et al. (2011), Calabrese et al. (2013) and Schwarz et al. (2006). The atlas generated by Valdés-Hernández et al. includes a digitalization of 96 cortical structures of the sixth edition of the Paxinos and Watson (P & W) atlas (George and Charles 2007). We included 24 subcortical structures from the atlas (Calabrese et al. 2013). We also included 6 other cortical structures, including the bilateral prelimbic cortex, the frontal association cortex, and the orbitofrontal cortex from the Schwarz atlas. The template from Calabrese et al. (2013) and Schwarz et al. (2006) was separately coregistered to the Valdés-Hernández atlas, which is in the MDT space. The combined atlas was then masked by the group-averaged brain mask, which was generated from the resting-state fMRI data, resulting in 110 brain regions.

For each animal, we extracted the averaged resting-state time course from each brain region. From the forepaw stimulation data, we also extracted the averaged residual time courses resulting from the above GLM analysis. These extracted time courses were used separately to construct resting-state and stimulation-related functional brain networks. Specifically, for each animal, we computed pairwise Pearson correlations to form a correlation matrix. To improve normality, the correlation *r* values were Fisher transformed to *Z* scores. To remove weak correlations that might arise from physiological and/or scanner noise, we applied a threshold on the correlation matrices so that only the correlations whose corresponding *P* values passed a statistical threshold ($P < 0.05$) were retained. The false discovery rate (FDR) method was used to correct for multiple comparisons by setting the FDR level to 0.05. We also constructed a group-averaged brain network by averaging thresholded correlation matrices across animals, and only correlations that were significant in at least 50% of the group were considered (Supplementary Fig. 1).

Rich-Club Structure

Rich-club organization is characterized by the tendency of the highly connected network hubs that are densely interconnected. To define the rich-club structure in a weighted network, we first calculated the nodal strength of each node (i.e., the sum of the strength of the existing connections), and computed the rich-club coefficient as follows (Colizza et al. 2006):

$$\phi^w(s) = \frac{w_{>s}}{\sum_{l=1}^{E_{>s}} W_l^{rank}},$$

where $w_{>s}$ is the sum of the connectivity strength between nodes with nodal strength higher than *s*, $E_{>s}$ is the number of these connections, and W_l^{rank} is the sum of the top $E_{>s}$ strongest connections in the network. A normalized $\phi^w_{norm}(s)$ can be obtained by dividing $\phi^w(s)$ by $\phi^w_{rand}(s)$, where $\phi^w_{rand}(s)$ is computed as the averaged rich-club coefficient from 100 random networks preserving the same degree (i.e., the number of existing connections of a given node) and strength distribution. A network appears to have a rich-club organization if $\phi^w_{norm}(s) > 1$, for a continuous range of *s*. We also evaluated the statistical significance of the rich-club results by permutation testing. The distribution of $\phi^w_{rand}(s)$ yielded a null distribution of rich-club coefficients obtained from random networks. Using this null distribution, a *P* value was assigned to $\phi^w(s)$ at each *s* level by computing the percentage of $\phi^w_{rand}(s)$ that were greater than the observed rich-club coefficient. We used the Bonferroni method to correct multiple comparisons and set the α-levels to 0.0017 per test (0.05/tests performed).

The rich club was then selected as the brain regions with the strongest nodal strength (>mean + standard deviation of all regions), which corresponds to $s > 4.83$ where rich-club structure significantly presents.

Modularity

We accessed the modular or community structure of the rat network by applying the modularity analysis on the group-averaged brain network under resting state. The modularity analysis partitions a network into a set of modules with a high intramodular connectivity but a low intermodular connectivity. We adopted the well-established Newman algorithm (Newman 2006) to detect the network partition by optimizing the level modularity Q.

Communication Efficiency of Brain Regions

To assess the contribution to network communication of a given brain region, we measured betweenness centrality and participation coefficient (PC).

Betweenness centrality

Betweenness centrality characterizes the importance of a node for network communication by measuring the number of times it is passed by the shortest paths between all node pairs in the network. For a given node i, the betweenness centrality B_i is given by the following:

$$B_i = \sum_{jk} \frac{n^i_{j,k}}{l_{jk}},$$

where $n^i_{j,k}$ equals to 1 if the shortest path between nodes j and k pass through node i, otherwise, $n^i_{j,k}$ is zero. l_{jk} is the number of shortest path between nodes j and k.

Participation coefficient

Based on the modular partition, PC is computed using the following formula:

$$PC_i = 1 - \sum_{s=1}^{N_M} \left(\frac{k_{is}}{k_i}\right)^2,$$

where N_M is the number of modules and k_{is} is the sum of connections between the node i and module s. k_i is the sum of connections of node i to all other nodes in the N_M modules. PC measures how well the connections of a given node are evenly distributed across different modules of the network and nodes with higher PC indicate that they tend to be connectors linking their own module to the other modules.

Communication Cost of Brain Regions

To communicate between brain regions, the neural system needs wiring and metabolic costs to build and to run. For a given brain region, we accessed its wiring cost of making anatomical connections to the rest of brain by computing averaged physical distance between its connected brain regions. The physical distance between 2 connected regions was approximated by computing the Euclidean distance between the regional centroids. For a given region, we also evaluated the metabolic cost for communicating with other brain regions by quantifying the average rCBF from the preprocessed ASL data.

Path Motifs

We studied the information-transfer pattern in the rat brain functional network by accessing the topological properties of network connections and shortest paths. The identification of rich-club members allows for the classification of connections into 3 topological categories, including rich-club connections connecting the rich-club nodes, feeder connections connecting rich-club members to peripheral nonrich-club nodes and local connections connecting nonrich-club regions (van den Heuvel et al. 2012).

On the basis of the connection categories, we can further investigate the information-transfer topology along the shortest path between 2 brain regions. Following the definition of van den Heuvel et al. (2012), the order of topological categories of the connections that traveled by the shortest path between 2 regions delineates the classes of paths, that is, path motifs. By studying the shortest path between any pair of regions, we identified all path motifs in the rat brain network and recorded the number of occurrences for each path motif. For example, the path motif of L-F-R indicates that the information flows between a peripheral node and a rich-club node first through a local connection, then a feeder connection and then a rich-club connection.

To evaluate the significance of path motifs, we compared rat brain network with an ensemble of 100 randomized networks with the same degree and strength distribution and computed the significance profile (SP) (Milo et al. 2004) for path motifs. First, for a given path motif i , we calculated the Z score as:

$$Z_i = \frac{N_i^{real} - <N_i^{rand}>}{std(N_i^{rand})},$$

where N_i^{real} is the number of times the given path motif appears in the network, and $<N_i^{rand}>$ and $std(N_i^{rand})$ are the mean and standard deviation of its occurrence in the randomized networks. The SP of a network is a vector of Z scores normalized to the unit length:

$$SP_i = \frac{Z_i}{(\sum Z_i^2)^{1/2}},$$

where negative SP_i values indicate underrepresented path motifs, while positive ones, especially those close to 1, represent significant path motifs. The SP offers a histogram of path motifs over a network, which allows comparison of path motif structure across networks.

For a given path motif, the 100 randomization of the brain network also provided a null distribution of motif count in a network with a random topology. Using this null distribution, we assigned a P value to each path motif, as the percentage of random values that exceeded the path motif count in the brain network.

Following the same schemes, we also accessed the topological classes of connections and shortest paths that connecting regions within a single module or from different modules.

Results

Rich-Club Organization in the Rat Brain Functional Networks

We explored the intrinsic functional architecture of whole-brain networks by exploiting resting-state fMRI in a group of rats. As shown in Figure 1A, rich-club organization was evident in functional brain architecture of rats, with an increasing normalized rich-club coefficient $\phi_{norm}(s) > 1$ for a range of s from 2.11 to 4.83 ($P < 0.05$, Bonferroni corrected).

The identified rich club was distributed widely across the rat brain (Fig. 1B, Table 1), including regions in the cingulate cortex (cg1 and cg2), retrosplenial cortex, prelimbic cortex (PrL), frontal cortex (Area 3), primary auditory cortex, insular cortex (IC), and olfactory cortex (OFC). The resulting functional rich-club regions, especially the frontal areas, were moderately overlapped with structural hubs (Supplementary Fig. 2), which were identified using the anatomical rat connectome data from the open-access BAMS-II connectivity database (Bota et al. 2015).

Using a modularity analysis (Newman and Girvan 2004; Newman 2006), the rat brain network was decomposed into 7 functionally segregated modules, comprising the putative default mode network (DMN), insular (IC), somatomotor, temporal/parietal (TP), thalamus, striatal and olfactory (OLF) regions (Fig. 1C).

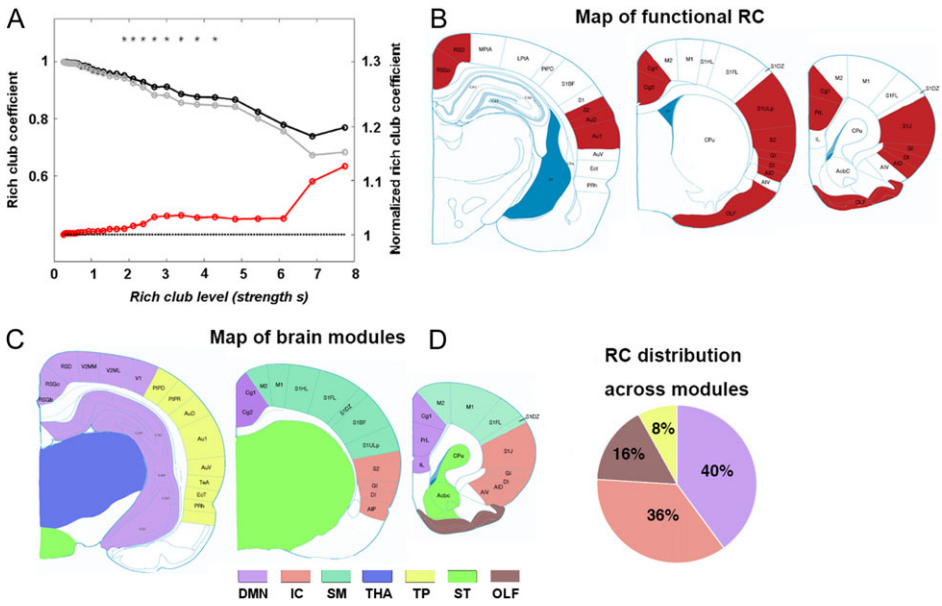

Figure 1. (*A*) The weighted rich-club coefficient values for a range of strength *s* are shown for the rat functional connectome (black line) and random networks (gray line, averaged across 100 comparable random networks). The normalized rich-club coefficients $\phi_{norm}(s)$ are also shown (red line). The rich-club curve suggests a significant rich-club organization of the rat functional connectome for a range of *s* from 2.11 to 4.83 (*$P < 0.05$, Bonferroni corrected). (*B*) Map of rich-club (RC) regions in resting-state functional brain networks of rats. (*C*) Module structure of rat functional connectome with brain regions color-coded according to their modular affiliation. (*D*) RC regions were found to be distributed across 4 brain modules as depicted in the pie graph, with a large percentage of hubs (40%) belonging to the DMN. SM, somatomotor areas; THA, thalamus; TP, temporal/parietal areas; ST, striatum areas; OLF, olfactory cortex.

Table 1 Brain regions comprising rich clubs of the rat functional brain networks

ROI label	Strength	Betweenness	Participation coefficient	Averaged distance	rCBF	Module ID
Right Cg1	9.76	0.029	0.44	5.07	51	DMN
Left Cg1	8.90	0.028	0.45	4.94	51	DMN
Right PrL	8.40	0.026	0.58	4.97	78	DMN
Left PrL	8.23	0.022	0.59	4.73	73	DMN
Right OFC	8.17	0.052	0.68	5.28	75	OLF
Right GI	8.08	0.009	0.069	6.79	52	IC
Left OLF	8.07	0.041	0.68	5.52	70	OLF
Left GI	7.99	0.005	0.052	6.92	45	IC
Right RSD	7.83	0.030	0.21	3.82	56	DMN
Left RSD	7.81	0.023	0.20	3.98	51	DMN
Right OLF	7.73	0.042	0.68	4.89	71	OLF
Right RSG	7.73	0.017	0.26	3.80	72	DMN
Right DI	7.40	0.016	0.09	6.46	53	IC
Right S1J	7.39	0.004	0.05	6.36	47	IC
Left OFC	7.33	0.044	0.68	5.94	68	OLF
Right Cg2	7.10	0.014	0.34	4.17	66	DMN
Right S1ULp	7.01	0.025	0.24	6.72	51	IC
Left AI	7.00	0.011	0.06	6.14	58	IC
Right S2	6.96	0.016	0.12	7.30	50	IC
Left Cg2	6.83	0.016	0.35	4.04	57	DMN
Left DI	6.82	0.017	0.06	6.53	52	IC
Left Au1	6.80	0.034	0.51	7.40	65	AUD
Left RSGc	6.62	0.018	0.24	3.65	60	DMN
Left Fr3	6.54	0.014	0.18	5.99	41	IC
Left AuD	6.27	0.040	0.57	6.10	45	AUD

Abbreviations: GI, granular insular cortex; RSD, retrosplenial dysgranular cortex; RSG, retrosplenial granular cortex; RSGc, retrosplenial granular cortex, c region; AuD, secondary auditory cortex, dorsal area; AI, agranular insular cortex; DI: dysgranular insular cortex.

The rich-club regions showed a diverse distribution among multiple modules, which were primarily located in 4 out of 7 modules, with 40% in the DMN, 36% in the IC, 16% in the OLF, and 8% in the TP module (Fig. 1*D*), indicating their importance in transferring and integrating information across modules.

Rich-Club Regions Are Highly Centralized and Highly Costly

Compared with the nonrich-club regions, rich-club regions appeared to show higher strength ($P < 0.001$, Fig. 2*A*). Also,

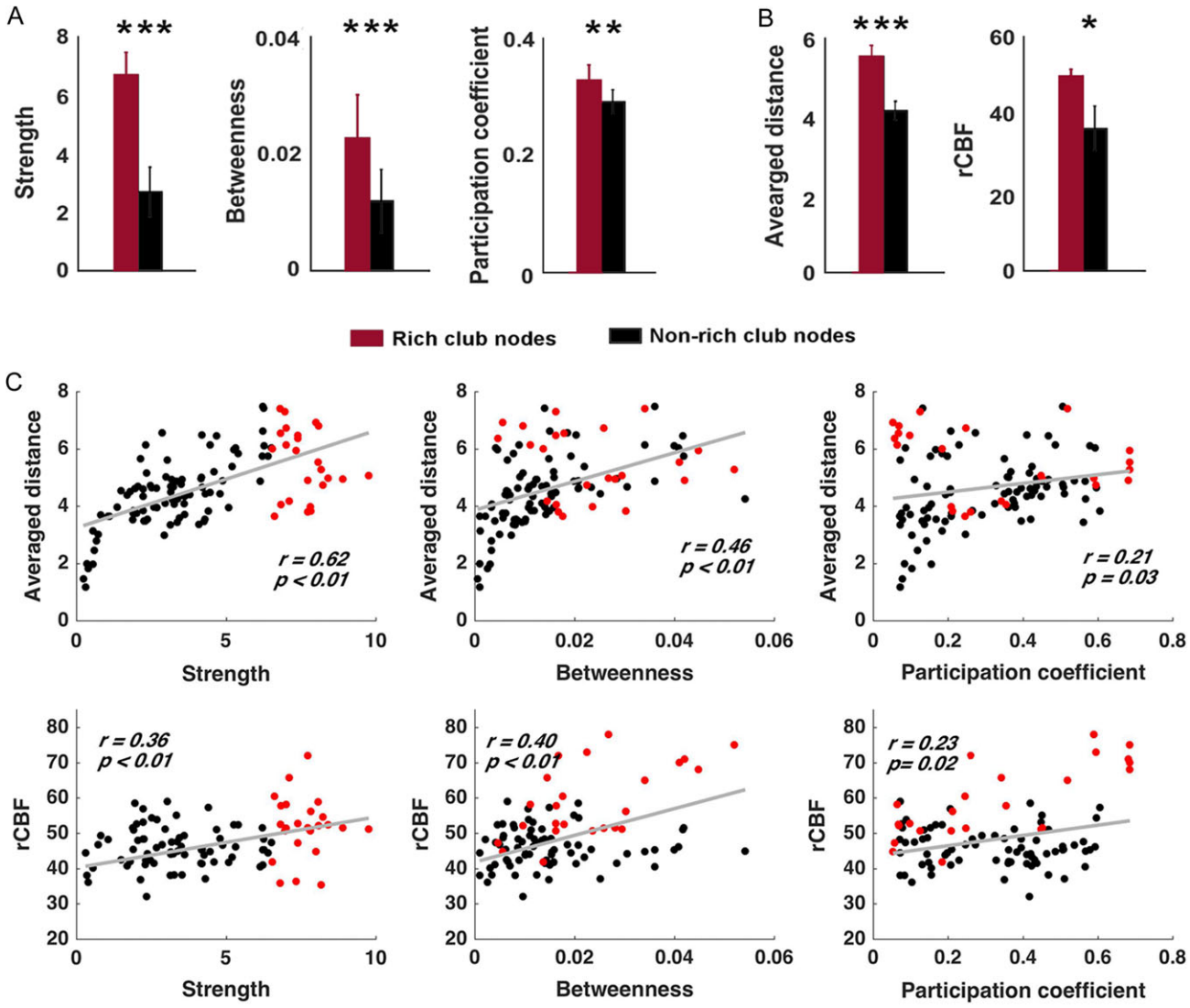

Figure 2. (*A*) Topological performance of rich-club and nonrich-club regions. Bar graphs show that the nodal strength, averaged functional connectivity, betweenness centrality and PC of rich-club nodes were significantly higher than those of nonrich-club ones. (*B*) Wiring and running cost of rich-club and nonrich-club regions. Bar graphs show the averaged physical distance (left panel) and the rCBF of rich-club and nonrich-club nodes, with rich-club nodes displaying a significantly longer wiring distance as well as higher rCBF supply as compared with nonrich-club nodes. ***$P < 0.001$; **$P < 0.01$; *$P < 0.05$.

rich-club regions exhibited higher betweenness centrality ($P < 0.001$), which indicates their central role in global information transfer in that most of the shortest paths between brain regions need to pass through the rich-club members in the rat functional brain network. Rich-club regions were also distinguished by showing higher PC ($P < 0.005$), indicating that they tend to serve as network connectors to communicate more with brain regions in different modules.

We next examined the wiring cost and running cost of rich-club regions (Fig. 2*B*). Wiring cost was accessed by computing the averaged physical distance (Euclidean distance) of a given region to the rest of the brain regions, while the running cost was evaluated by the rCBF measured from ASL perfusion imaging in a separate group of rats ($n = 8$). Compared with the nonrich-club regions, the rich club was costlier in terms of both wiring distance ($P < 0.001$) and rCBF supply ($P = 0.02$). Scatter plots of wiring/running cost against topological metrics are shown in Figure 2*C*. The significant high correlations between communication cost and efficiency suggest a tendency of the neural system to invest costly resources for a facilitation of topologically efficient information transfer and integration.

Rich-Club Bridges Information Transfer in Rat Brain Networks: From Connections to Paths

We then characterized the information-transfer patterns in functional networks of the rat brain. Two brain regions can communicate to each other through a direct connection, which can be categorized into 3 topological types (van den Heuvel et al. 2012) (Fig. 3*A*): 1) rich-club connections (R), connecting rich-club regions; 2) feeder connections (F), connecting rich club with poor periphery regions; and 3) local connections (L) connecting periphery regions. Connections that pass through rich-club regions accounted for a relatively high percentage (totally 55%; rich-club and feeder connections 14% and 41%, respectively) of all connections across the whole-brain network (Fig. 3*B*). A similar connection pattern was observed in

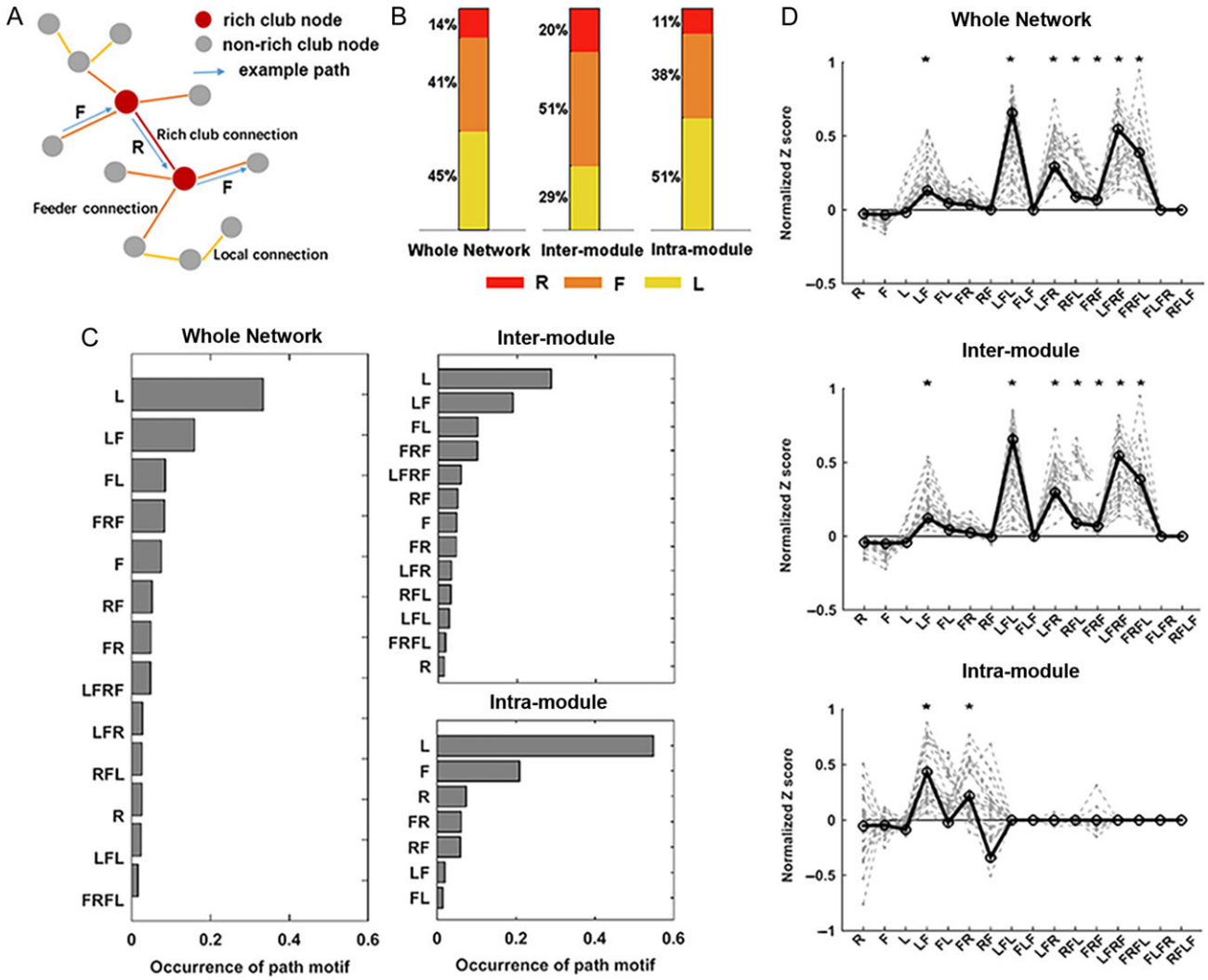

Figure 3. (*A*) Schematic illustration of path motif and local (L), feeder (F), and rich-club (R) connections. (*B*) Proportions of local, feeder, and rich-club connections contributing to whole network, intermodule, and intramodule communications. (*C*) The percentage occurrence of path motifs of all shortest paths connecting regions across the whole network, between modules and within single modules, respectively. (*D*) The significance profiles are plotted as normalized significance level (Z score) of path motifs of all shortest paths connecting regions across the whole network, between modules and within single modules, respectively (*$P < 0.05$, Bonferroni corrected). Solid lines are significance profiles for group-averaged brain network, whereas dashed lines represent significance profiles for each individual rat brain network.

intermodule connections, where rich-club and feeder connections constituted 20% and 51%, respectively, of all such connections, indicating their important role in integrating information between different brain modules. In contrast, local connections were dominant (51%) in connecting intramodule brain regions with rich-club and feeder connections accounting for 11% and 38%, respectively.

We next explored the information-transfer chains by analyzing the shortest paths between brain regions. The shortest paths can travel through multiple connections between a pair of regions, and the order of the topological types of these connections defines the "path motifs" (Fig. 3A), a class of paths to which each information-transfer chain belongs (van den Heuvel et al. 2012). For example, the path motif of F-R-F indicates that the information flows between 2 peripheral nodes first through a feeder connection, then a rich-club connection and then another feeder connection (Fig. 3A). We recorded the number of occurrences of each path motif in the rat brain functional network. We found that although the most frequent path motif was the "L" motif that traveled only through periphery nodes (Fig. 3C, left panel), the path motifs appearing in the rat brain network at significantly higher frequencies than those in the random networks ($n = 100$) were those travelling through rich-club regions and connections to pass information between periphery regions, including L-F, L-F-L, L-F-R, R-F-L, F-R-F, L-F-R-F, and F-R-F-L (Fig. 3D, left panel). A similar pattern of the information-transfer chains was also observed in the shortest paths between intermodule brain regions (Fig. 3C, upper right panel; and Fig. 3D, middle panel). As for communications within modules, we found that the length of shortest paths was relatively shorter than intermodule paths, and the most frequent path motif was also the "L" motif (Fig. 3C, lower right panel). Nevertheless, path motifs of "L-F" and "F-R," which needed to transfer information via a rich-club region, were found to have significantly higher frequencies than those in the random networks (Fig. 3D, right panel). Finally, we also plotted the significance profiles of path motifs for each individual rat (dotted lines, Fig. 3D), demonstrating that the

observations of significant path motifs replicate well even in individual rats. These results indicate that although the "L" motif occurs the most between regions within and between different modules, the path motifs that involve rich-club nodes and connections distinguish the rat brain network from random networks and might underlie efficient information communication.

Reorganization of Rich-Club Structure During Electrical Forepaw Stimulation

To explore whether and how the topological organization of the rat brain functional network would dynamically reconfigure when the animals experienced external stimulation, we explored the potential alterations in rich-club structure, spatial distribution, as well as information-transfer patterns of the rat brain network during forepaw (left) electrical stimulation.

As expected, during forepaw stimulation, rat brain networks exhibited preserved rich-club organization as expressed by the above-random rich-club coefficient for $s = 4$ to $s = 7$ ($P < 0.05$, Bonferroni corrected) (Supplementary Fig. 3A). There was no significant difference in rich-club coefficient at any s level when comparing with resting-state brain networks (all Ps > 0.05, permutation tests). In addition, we did not find any significant stimulation-induced changes in the distribution of rich-club, feeder, or local connections.

During forepaw stimulation, rich-club regions appeared to show high consistency compared with those found in resting-state brain networks (Supplementary Fig. 3B). However, we found that the right primary somatosensory cortex forelimb region (S1FL), which was significantly activated by forepaw stimulation ($P < 0.0001$, corrected, Supplementary Fig. 4A), showed significantly decreased connectivity strength ($t = -3.05$, $P < 0.005$, paired t-tests, uncorrected, Supplementary Fig. 4A). Unfolding the functional connectivity profile of the right S1FL (Supplementary Fig. 4C), we found that this region exhibited weaker temporal synchronization with a variety of brain regions except its anatomical neighbor, the right primary somatosensory cortex dysgranular zone (S1DZ) (all Ps < 0.05, uncorrected). More interestingly, we found that the decreased functional strength in the right S1FL correlated negatively with stimulation activation in that region ($r = -0.45$, $P = 0.017$) (Supplementary Fig. 4B).

Forepaw stimulation also induced extensive changes in information-transfer pattern across the whole-brain network ($P < 0.01$, permutation test, Bonferroni corrected). While the occurrence of "L" type path motif increased significantly, path motifs that involve the rich-club regions or connections, including the "L-F-L," "F-R-F," "L-F-R-F," and "F-R-F-L," were found to be less recruited during forepaw stimulation (Fig. 4A, upper panel). Similar findings were also observed for intermodule path motifs (Fig. 4A, lower panel). No significant changes were found in intramodule path motifs. We then examined

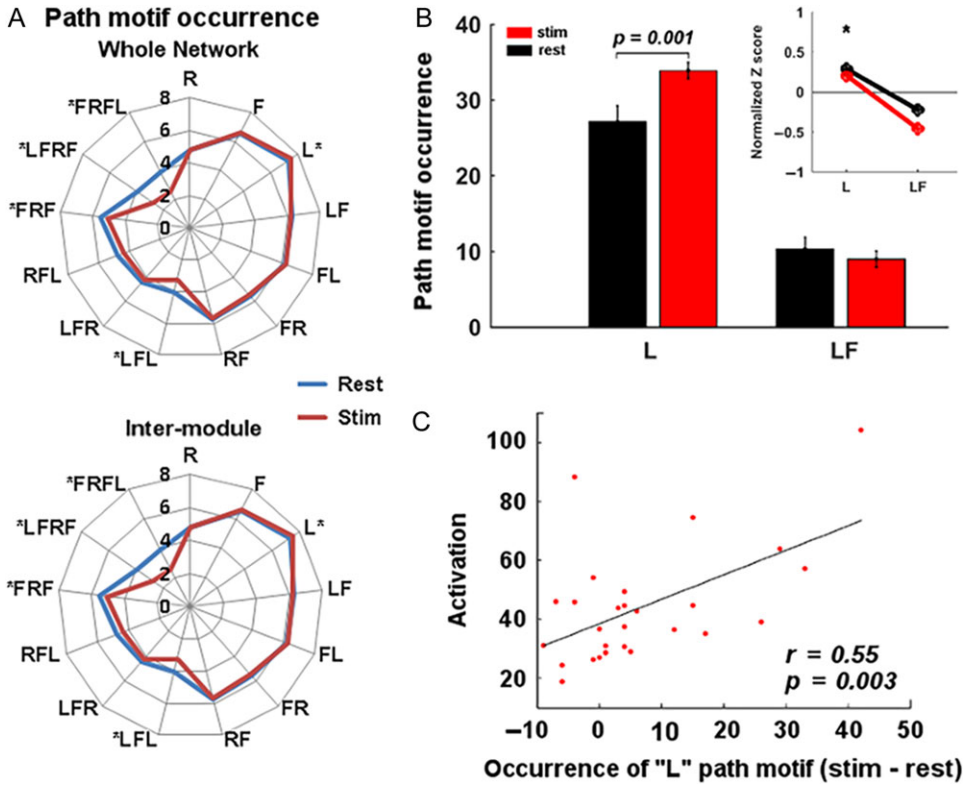

Figure 4. Forepaw stimulation effects on rich-club organization of rat functional brain network. (A) Fingerprint of path motif occurrence of whole-brain network and intermodule communications during both resting and forepaw stimulation states. Path motif occurrences are shown as their log values for easier visualization. *$P <$ 0.05, Bonferroni corrected. (B) The occurrences of the 2 existing kinds of path motifs, "L" and "LF," of the shortest paths connecting the right S1FL are plotted for both resting and forepaw stimulation states. The inset plot shows the normalized significance level (Z score) of the 2 path motifs comparing with random networks, and only the "L" path motif is found to occur significantly more than that in random networks during both resting and stimulation states ($P < 0.01$, Bonferroni corrected). In comparison to at resting state, the "L" motif occurs significantly more frequently during the forepaw stimulation ($P = 0.001$, permutation test). (C) The increased occurrence of the "L" motif correlated significantly with the stimulation-induced activation in right S1FL.

specifically the path motifs connecting stimulation-activated right S1FL to other brain regions, and found 2 types of path motifs, the "L" and "L-F" motifs, and one of them, the "L" motif appeared significantly more frequently than in random networks (Fig. 4B, inset plot). During forepaw stimulation, the "L" motif was found to occur significantly more frequently (P = 0.001, permutation test), while occurrence of the "L-F" motif stayed relatively unchanged (Fig. 4B). Moreover, we further observed that the increased occurrence of the "L" motif was correlated with stimulation-induced activation in right S1FL (r = 0.55, P = 0.003) (Fig. 4C).

Validation Analysis

While comparing the networks between the resting and stimulation states, all the above analyses were based on brain networks thresholded at a specified statistical significance level ($P < 0.05$, FDR corrected), which could result in different number of suprathreshold connections in brain networks between states, and may thus contribute to the stimulation-induced differences in network topology we observed. Therefore, as a validating analysis, we also constructed rat brain networks by using a sparsity threshold (15% topmost connections preserved), which ensures the same number of suprathreshold connections for both states. All of the above results were replicated for the sparsity-thresholded rat brain networks (Supplementary Fig. 5), indicating the reliability of our results and ruling out any potential confounding effect of different number of connections between resting and stimulation state.

To assess the reproducibility of the forepaw stimulation effects on path motifs, we divided the subjects into 2 subgroups randomly for 500 times, and for each split, we performed the statistical analyses for each subgroup to compare path motif occurrence between resting and stimulation states. Then for any path motif class that shows significant stimulation-induced differences in our main analyses, we computed its reproducibility as the number of significant comparisons over all the split subgroups, normalized by the number of 1000 (500 × 2) subgroups; in contrast, for path motif class with no significant stimulation-induced changes observed in our main analyses, we computed its reproducibility as the number of nonsignificant comparisons over all the split subgroups, normalized by the number of 1000 subgroups. Our results showed high reproducibility of the stimulation effects on the occurrence of the whole-brain network path motifs, and the intermodule path motifs (Supplementary Fig. 6A, right panel). The stimulation-induced alterations appear to show a similar pattern as those in the main analyses, where "L" type path motif significantly increased, and the "L-F-L," "F-R-F," "L-F-R-F," and "F-R-F-L" path motifs occurred less during forepaw stimulation (Supplementary Fig. 6A, left panel). As for the path motifs connecting stimulation-activated right S1FL to other brain regions (Supplementary Fig. 6B), we found significantly more "L" motif during stimulation with a high reproducibility of 75.5%, while the "L-F" motif stayed relatively unchanged over most split subgroups (93.5% reproducibility).

Discussion

In this study, we demonstrated the existence of rich-club organization of functional brain networks in rats, with densely interconnected rich-club regions being distributed predominately within the putative DMN. Rich-club regions exhibited high wiring cost as well as high metabolic cost, which may have evolved to achieve high network communications to support efficient brain function. These observations are in agreement with the rich-club findings reported for structural brain networks in rodents and other species (Harriger et al. 2012; van den Heuvel et al. 2012, 2015; de Reus and van den Heuvel 2013; Towlson et al. 2013), suggesting that rich-club architecture is a common feature across species, and optimizes the balance between communication cost and communication efficiency. We further assessed the modulation of topological architecture of the rat brain during forepaw electrical stimulation and revealed that functional brain architecture reorganized its topological routes by increasing local shortcuts but decreasing the path motifs involving rich-club members. The activated somatosensory region in the S1FL also showed increased local shortcuts, which predicted the magnitude of its stimulation-induced activation.

In functional brain networks of rats, we discovered a set of hubs that were densely interacted. Part of these hubs (48%), including the cingulate, retrosplenial and prelimbic regions, represent a spatial ensemble of key areas in the putative DMN (Lu et al. 2012), which is consistent with recent findings in rodents (Liska et al. 2015; Ma et al. 2016) and the hub distribution typically observed in human studies (Buckner et al. 2009; van den Heuvel and Sporns 2011; van den Heuvel et al. 2012; Liang et al. 2013). We found additional hubs in the functional network of the rat brain located in multiple brain modules, including the IC, OFC, and auditory cortex. The functional hub distribution in rat brain largely resembles the findings in a recent study in awake rats (Ma et al. 2016), suggesting high reproducibility of the functional hubs in rat brain regardless of the different anesthetize schemes or analytic approaches. We have also qualitatively compared functional and structural hub distribution, which appeared to be moderately overlapped, predominately in frontal regions, including the anterior cingulate, prelimbic frontal, and orbital frontal areas, indicating their topological significance in both structural and functional brain networks. In contrast, functional hubs in the retrosplenial and insular cortices and structural hubs in the entorhinal cortices were not overlapped with the other. Such discrepancies could be a reflection of different topological roles that a brain region may play in functional and anatomical connectome. However, further studies are warranted to quantitatively compare functional and structural rich-club distributions of the rat brain in the same brain atlas. Our results also indicate a spatially scattered distribution of hubs across multiple brain modules, which has been shown in brain networks of other species (Harriger et al. 2012; de Reus and van den Heuvel 2013), suggesting an essential characteristic to facilitate intermodule communications supporting multifunction integration. Topologically, we reaffirmed that hubs from various modules are densely interconnected to form a "rich club," which is another significant feature to provide express communications needed to disperse and integrate information efficiently, and exert vital influence on the entire network. These spatially distributed, while topologically connected, brain hubs, consisting of DMN, insula, and sensory-related regions of auditory and olfactory cortices, may represent a functional processing core in the rat brain required to respond to internal and external contingencies. The rich-club phenomenon has been observed across a range of different species (van den Heuvel et al. 2016). The consistent presence of rich-club organization suggests a general topological principle of neural systems to centralize connections into a connective core, which may facilitate information coordination and integration to support higher order brain functions.

We evaluated communication efficiency of rich-club regions in the rat brain network by computing their betweenness centrality and PC. Comparing with peripheral regions, we found that rich-club regions had higher betweenness as well as higher PC. Betweenness centrality measures the extent to which a node lies on the geodesic paths between others (Brandes 2001), while the PC indices how the connections of a node are well distributed among different modules (Guimera and Amaral 2005a, 2005b). Therefore, with higher betweenness and participation index, rich-club members could facilitate the spread of information between different brain regions and modules in the rat brain network. Another line of evidence supporting rich-club regions as central integrators in the rat brain network comes from the examination of the connections and information-transfer pathways they have formed. Compared with local connections that link nonrich-club nodes, rich-club and feeder connections accounted for a relatively small proportion of intramodule communications. In contrast, they showed a clear prevalence when information was transferred between different modules. Moreover, comparing with random networks preserving the same degree and strength distribution but without a rich-club topology, we found that both rich-club and feeder connections are well represented among intermodule paths in the rat brain network, connecting peripheral regions through organized sequences that feed the information from peripheral nodes into rich-club regions and then transfer to another local region. Note that rather than a complete chain of L-F-R-F-L observed in human (van den Heuvel et al. 2012) and macaque (Harriger et al. 2012) anatomical brain networks, a series of its subpath motifs were found in the rat brain instead, including L-F-R, R-F-L, F-R-F, L-F-R-F, and F-R-F-L. There were no long paths greater than 4 steps in the current rat functional brain network, which might be due to the relatively small overall size and/or specific regions such as prefrontal cortex in the rat brain. Rat brain network has been shown to possess "small-world" properties (Watts and Strogatz 1998; Liang et al. 2011, 2012), which has short path length similar to comparable random networks, to enable efficient global information transfers. Our findings of overrepresented path motifs involving rich-club and feeder connections in the rat brain, relative to random networks, suggest that the rat brain paves express pathways using strategies different from random networks. In the rat brain, efficient paths are routed to cross the central rich-club system, in a way that not only promotes network efficiency, but also integrates, processes, and propagates neuronal information across segregated regions to achieve various brain functions (Bassett et al. 2009; van den Heuvel et al. 2009; Kitzbichler et al. 2011; Baggio et al. 2015).

Comparing with nonrich-club nodes, we found that rich-club regions had longer wiring distance, which is in concordance with previous findings that rich-club connections usually span long distances and impose high wiring cost on constructing and maintaining the brain architecture (Collin et al. 2014b). More importantly, we also showed that the rich-club regions were supplied with larger metabolic resources indicated by higher CBF, suggesting that rich-club members tend to consume more energy and require a high running cost. Earlier findings from structural studies suggested that the rich-club organization might be the result of an optimal balance between minimization of wiring cost and maximization of communication efficiency (Kaiser and Hilgetag 2006; van den Heuvel et al. 2012). We have observed a similar phenomenon of high topological performance as well as high wiring cost for rich-club members in functional brain network of rats, suggesting that the same principle also applies to organizing the functional operations embedded in the structural circuits (Vértes et al. 2012). Moreover, our finding of high CBF among rich-club regions indicates that brain networks are organized with consideration to not only the wiring cost for building and maintaining the network, but also the metabolic cost for running and operation (Bullmore and Sporns 2012; Liang et al. 2013).

Another noteworthy observation is that, although underrepresented comparing to random networks, local path motifs that cross only nonrich-club regions showed the highest occurrence, especially for intramodule communications in the rat brain. In contrast to previous structural network studies in which local path motifs were usually not among the highest occurring motifs (van den Heuvel et al. 2012; de Reus and van den Heuvel 2013), the excessive local routes in functional brain networks may indicate that they could be of high importance in efficiently processing domain-specific local neuronal information when the brain system is dynamically operating (Alexander-Bloch et al. 2010; Sepulcre et al. 2010; Alexander-Bloch et al. 2013). Moreover, the existence of local connections and path motifs may offset the elevated energy budget raised by the rich-club system, and thus play a vital role in minimizing the running cost and reducing energy-demanding pressure in rat functional brain network (Niven and Laughlin 2008).

To understand the functional roles that such topological features play in the rat brain, it is important to understand how they would dynamically reconfigure in response to external stimulations. Given the unimodal nature of the simple forepaw stimulations used in the current study, it would be expected that the modulation effects would be localized within the site relevant to the somatosensory stimulation. Our results partially support the above expectation. First, during forepaw stimulation, the rich-club organization, as indicated by the rich-club coefficient, was found to remain almost the same as in the resting in rat functional network, suggesting a preservation of such global topological features when experiencing external stimulation. Second, we found that the spatial distribution of rich-club regions was also preserved during the forepaw stimulation, and the stimulation effect on nodal strength could only be detected at the right S1FL, which is exactly the same region activated by the stimulations (Zhao et al. 2008). The right S1FL exhibited decreased functional connectivity strength, which may reflect its reduced synchronization with other brain regions that were mostly unresponsive to the specific somatosensory stimulation. This finding is in concordance with a recent study showing significantly decreased bilateral whisker barrel cortex connectivity during unilateral continuous whisker stimulation (Lu et al. 2014). However, when probing information-transfer pattern along the shortest paths that could pass through multiple connections between 2 regions, we found that the forepaw stimulation can induce extensive reorganization of path motifs across the whole-brain network. The increased occurrence of "L" motif is accompanied with significantly reduced number of rich-club member-involved path motifs, which may help to conserve metabolic running cost and keep the energy budget under control during forepaw stimulation. Such stimulation effects may have been transmitted through the multimodal association region of medial agranular cortex, which ties strongly to the somatosensory cortex, and passed over to the whole network through its rich connections with key DMN structures, including the anterior cingulate and retrosplenial regions (Reep et al. 1990). Examining the path motifs particularly linking the stimulation-activated region of the right S1FL, we found that the "L" path motif tended to appear more during stimulation.

"L" and "L-F" motifs were the only 2 path motifs that existed for the right S1FL, and "L" motif was the only one that showed significantly more occurrence over random networks, indicating that a peripheral somatosensory region, such as the right S1FL here, may transfer and process information by taking mainly the local routes, while also reaching out to rich-club regions through the "LF" path motifs. During forepaw stimulation, the right S1FL region increased its "L" motif to focalize its resources to receive and process the stimulation in a cost-efficient way.

Of note, the animals were anesthetized in our study to facilitate fMRI experiments. It has been shown that fMRI signal appears to be anesthetic dependent across multiple species (Grandjean et al. 2014; Barttfeld et al. 2015) including rats (Liu et al. 2013). However, experiments conducted by ours and other groups have demonstrated that the combined use of (dex) medetomidine and isoflurane maintains both stable sedation and strong functional connectivity within cortical and subcortical structures in rodents (Lu et al. 2012; Grandjean et al. 2014). Nevertheless, we cannot rule out the possibility that fMRI signals were affected by anesthesia, and future studies will be needed to reproduce our current observations in awake rats.

In conclusion, we demonstrate the existence of the rich-club architecture in functional brain networks of rats. By examining its topological performance as well as the physical and metabolic cost, our results suggest that the principle of balancing between minimizing wiring/running cost and maximizing communication efficiency applies to the functional network during spontaneous operation of the neuronal system. When experiencing electrical forepaw stimulation, rat functional brain networks respond by recruiting local paths connecting only nonrich-club regions to the activated somatosensory area, which further reinforces the principle that the brain operates in a way to achieve its goals with minimal energy expenditure.

Supplementary Material

Supplementary material are available at *Cerebral Cortex* online.

Funding

The Intramural Research Program of the National Institute on Drug Abuse, National Institutes of Health, the Natural Science Foundation of China (Grant Nos. 81671769, 91432115, and 81225012), Changjiang Scholar Professorship Award (Award No. T2015027) and the Beijing Natural Science Foundation (Grant No. Z151100003915082).

Notes

Conflict of Interest: None declared.

References

Alexander-Bloch AF, Gogtay N, Meunier D, Birn R, Clasen L, Lalonde F, Lenroot R, Giedd J, Bullmore ET. 2010. Disrupted modularity and local connectivity of brain functional networks in childhood-onset schizophrenia. Front Syst Neurosci. 4:147.

Alexander-Bloch AF, Vértes PE, Stidd R, Lalonde F, Clasen L, Rapoport J, Giedd J, Bullmore ET, Gogtay N. 2013. The anatomical distance of functional connections predicts brain network topology in health and schizophrenia. Cereb Cortex. 23:127–138.

Baggio HC, Segura B, Junque C, de Reus MA, Sala-Llonch R, Van den Heuvel MP. 2015. Rich club organization and cognitive performance in healthy older participants. J Cogn Neurosci. 27:1801–1810.

Barttfeld P, Uhrig L, Sitt JD, Sigmane M, Jarrayaa B, Dehaenea S. 2015. Signature of consciousness in the dynamics of resting-state brain activity. Proc Natl Acad Sci USA. 112:887–892.

Bassett DS, Bullmore ET, Meyer-Lindenberg A, Apud JA, Weinberger DR, Coppola R. 2009. Cognitive fitness of cost-efficient brain functional networks. Proc Natl Acad Sci USA. 106:11747–11752.

Bota M, Sporns O, Swansona LW. 2015. Architecture of the cerebral cortical association connectome underlying cognition. Proc Natl Acad Sci USA. 112:E2093–E2101.

Brandes U. 2001. A faster algorithm for betweenness centrality. J Math Sociol. 25:163–177.

Buckner RL, Sepulcre J, Talukdar T, Krienen FM, Liu H, Hedden T, Andrews-Hanna JR, Sperling RA, Johnson KA. 2009. Cortical hubs revealed by intrinsic functional connectivity: mapping, assessment of stability, and relation to Alzheimer's disease. J Neurosci. 29:1860–1873.

Bullmore E, Sporns O. 2009. Complex brain networks: graph theoretical analysis of structural and functional systems. Nat Rev Neurosci. 10:186–198.

Bullmore E, Sporns O. 2012. The economy of brain network organization. Nat Rev Neurosci. 13:336–349.

Calabrese E, Johnson GA, Watson C. 2013. An ontology-based segmentation scheme for tracking postnatal changes in the developing rodent brain with MRI. Neuroimage. 67:375–384.

Colizza V, Flammini A, Serrano MA, Vespignani A. 2006. Detecting rich-club ordering in complex networks. Nat Phys. 2:110–115.

Collin G, Kahn RS, de Reus MA, Cahn W, van den Heuvel MP. 2014a. Impaired rich club connectivity in unaffected siblings of schizophrenia patients. Schizophr Bull. 40:438–448.

Collin G, Sporns O, Mandl RC, van den Heuvel MP. 2014b. Structural and functional aspects relating to cost and benefit of rich club organization in the human cerebral cortex. Cereb Cortex. 24:2258–2267.

Cox RW, Hyde JS. 1997. Software tools for analysis and visualization of fMRI data. NMR Biomed. 10:171–178.

Dai Z, Yan C, Li K, Wang Z, Wang J, Cao M, Lin Q, Shu N, Xia M, Bi Y, et al. 2014. Identifying and mapping connectivity patterns of brain network hubs in Alzheimer's disease. Cereb Cortex. 25:3723–3742.

de Reus MA, van den Heuvel MP. 2013. Rich club organization and intermodule communication in the cat connectome. J Neurosci. 33:12929–12939.

George P, Charles W. 2007. The rat brain in stereotaxic coordinates. 6th ed. London: Academic Press.

Grandjean J, Schroeter A, Batata I, Rudin M. 2014. Optimization of anesthesia protocol for resting-state fMRI in mice based on differential effects of anesthetics on functional connectivity patterns. NeuroImage. 102:838–847.

Guimera R, Amaral L. 2005a. Cartography of complex networks: modules and universal roles. J Stat Mech. 2:27–61.

Guimera R, Amaral L. 2005b. Functional cartography of complex metabolic networks. Nature. 433:895–900.

Harriger L, van den Heuvel MP, Sporns O. 2012. Rich club organization of macaque cerebral cortex and its role in network communication. PLoS One. 7:e46497.

Kaiser M, Hilgetag CC. 2006. Nonoptimal component placement, but short processing paths, due to long-distance projections in neural systems. PLoS Comput Biol. 2:e95.

Kitzbichler MG, Henson RN, Smith ML, Nathan PJ, Bullmore ET. 2011. Cognitive effort drives workspace configuration

of human brain functional networks. J Neurosci. 31: 8259–8270.
Liang X, Zou Q, He Y, Yang Y. 2013. Coupling of functional connectivity and regional cerebral blood flow reveals a physiological basis for network hubs of the human brain. Proc Natl Acad Sci USA. 110:1929–1934.
Liang X, Zou Q, He Y, Yang Y. 2015. Topologically reorganized connectivity architecture of default-mode, executive-control, and salience networks across working memory task loads. Cereb Cortex. 26:1501–1511.
Liang Z, King J, Zhang N. 2011. Uncovering intrinsic connectional architecture of functional networks in awake rat brain. J Neurosci. 31:3776–3783.
Liang Z, King J, Zhang N. 2012. Intrinsic organization of the anesthetized brain. J Neurosci. 32:10183–10191.
Liska A, Galbusera A, Schwarz AJ, Gozzi A. 2015. Functional connectivity hubs of the mouse brain. Neuroimage. 115:281–291.
Liu X, Zhu XH, Zhang Y, Chen W. 2013. The change of functional connectivity specificity in rats under various anesthesia levels and its neural origin. Brain Topogr. 26:363–377.
Lu H, Wang L, Rea WW, Brynildsen JK, Jaime S, Zuo Y, Stein EA, Yang Y. 2014. Low- but not high-frequency LFP correlates with spontaneous BOLD fluctuations in rat Whisker Barrel cortex. Cereb Cortex. 26:683–694.
Lu H, Zou Q, Gu H, Raichle ME, Stein EA, Yang Y. 2012. Rat brains also have a default mode network. Proc Natl Acad Sci USA. 109:3979–3984.
Ma Z, Perez P, Ma Z, Liu Y, Hamilton C, Liang Z, Zhang N. 2016. Functional atlas of the awake rat brain: A neuroimaging study of rat brain specialization and integration. Neuroimage. doi:10.1016/j.neuroimage.2016.07.007.
Milo R, Itzkovitz S, Kashtan N, Levitt R, Shen-Orr S, Ayzenshtat I, Sheffer M, Alon U. 2004. Superfamilies of evolved and designed networks. Science. 303:1538–1542.
Newman ME. 2006. Modularity and community structure in networks. Proc Natl Acad Sci USA. 103:8577–8582.
Newman ME, Girvan M. 2004. Finding and evaluating community structure in networks. Phys Rev E Stat Nonlin Soft Matter Phys. 69:026113.
Niven JE, Laughlin SB. 2008. Energy limitation as a selective pressure on the evolution of sensory systems. J Exp Biol. 211:1792–1804.
Reep RL, Goodwin GS, Corwin JV. 1990. Topographic organization in the corticocortical connections of medial agranular cortex in rats. J Comp Neurol. 294:262–280.
Rubinov M, Ypma RJ, Watsond C, Bullmore ET. 2015. Wiring cost and topological participation of the mouse brain connectome. Proc Natl Acad Sci USA. 112:10032–10037.
Schwarz AJ, Danckaert A, Reese T, Gozzi A, Paxinos G, Watson C, Merlo-Pich EV, Bifone A. 2006. A stereotaxic MRI template set for the rat brain with tissue class distribution maps and co-registered anatomical atlas: application to pharmacological MRI. Neuroimage. 32:538–550.
Senden M, Deco G, de Reus MA, Goebel R, van den Heuvel MP. 2014. Rich club organization supports a diverse set of functional network configurations. Neuroimage. 96:174–182.
Sepulcre J, Liu H, Talukdar T, Martincorena I, Yeo BT, Buckner RL. 2010. The organization of local and distant functional connectivity in the human brain. PLoS Comput Biol. 6: e1000808.
Sporns O. 2013. Network attributes for segregation and integration in the human brain. Curr Opin Neurobiol. 23:162–171.
Towlson EK, Vértes PE, Ahnert SE, Schafer WR, Bullmore ET. 2013. The rich club of the C. elegans neuronal connectome. J Neurosci. 33:6380–6387.
Valdés-Hernández PA, Sumiyoshi A, Nonaka H, Haga R, Aubert-Vásquez E, Ogawa T, Iturria-Medina Y, Riera JJ, Kawashima R. 2011. An in vivo MRI template set for morphometry, tissue segmentation, and fMRI localization in rats. Front Neuroinform. 5:26.
van den Heuvel MP, Kahn RS, Goñi J, Sporns O. 2012. High-cost, high-capacity backbone for global brain communication. Proc Natl Acad Sci USA. 109:11372–11377.
van den Heuvel MP, Scholtens LH, de Reus MA. 2015. Topological organization of connectivity strength in the rat connectome. Brain Struct Funct. 221:1719–1736.
van den Heuvel MP, Sporns O. 2011. Rich-club organization of the human connectome. J Neurosci. 31:15775–15786.
van den Heuvel MP, Sporns O. 2013a. An anatomical substrate for integration among functional networks in human cortex. J Neurosci. 33:14489–14500.
van den Heuvel MP, Sporns O. 2013b. Network hubs in the human brain. Trends Cogn Sci. 17:683–696.
van den Heuvel MP, Sporns O, Collin G, Scheewe T, Mandl RC, Cahn W, Goñi J, Hulshoff Pol HE, Kahn RS. 2013. Abnormal rich club organization and functional brain dynamics in schizophrenia. JAMA Psychiatry. 70:783–792.
van den Heuvel MP, Stam CJ, Kahn RS, Hulshoff Pol HE. 2009. Efficiency of functional brain networks and intellectual performance. J Neurosci. 29:7619–7624.
van den Heuvel MP, Bullmore ET, Sporns O. 2016. Comparative connectomics. Trends Cogn Sci. 20:345–361.
Vértes PE, Alexander-Bloch AF, Gogtay N, Giedd JN, Rapoport JL, Bullmore ET. 2012. Simple models of human brain functional networks. Proc Natl Acad Sci USA. 109: 5868–5873.
Watts DJ, Strogatz SH. 1998. Collective dynamics of 'small-world' networks. Nature. 393:440–442.
Zhao F, Zhao T, Zhou L, Wu Q, Hu X. 2008. BOLD study of stimulation-induced neural activity and resting-state connectivity in medetomidine-sedated rat. Neuroimage. 39: 248–260.